Lattice symmetry of the spiral spin-density-wave state in γ-Fe precipitates in Cu

Yorihiko Tsunoda, Hajime Nogami, and Masao Takasaka
School of Science and Engineering, Waseda University, 3-4-1, Ohkubo, Shinjuku, Tokyo 169-8555, Japan
(Received 13 February 2007; published 10 August 2007)

Lattice symmetry of γ-Fe in a spiral spin-density-wave (SDW) state was studied by neutron scattering experiments under uniaxial stress. If we express a wave vector of the spiral SDW as $\mathbf{q}_2=\mathbf{Q}_{AF}+\mathbf{Q}_{md}$, where $\mathbf{Q}_{AF}=(1,0,0)(2\pi/a)$ and $\mathbf{Q}_{md}=(0,\xi,0)(2\pi/a)$, the volume fraction of γ-Fe precipitates with the $\mathbf{Q}_{md}$ vector parallel to uniaxial stress increasing and that with the $\mathbf{Q}_{AF}$ vector decreasing under uniaxial stress, indicating that an fcc lattice contracts along the direction parallel to $\mathbf{Q}_{md}$ and expands along the $\mathbf{Q}_{AF}$ direction below the Néel temperature. The magnitude of the lattice distortion is estimated to be of the order of 10^{-4}, which would not suffice to explain the discrepancies between the experimental results and the first principles calculations assuming the ideal cubic lattice. Similarities of the lattice symmetry with CuMn spin-glass alloys are discussed.

DOI: 10.1103/PhysRevB.76.054419 PACS number(s): 75.80.+q, 75.25.+z, 75.30.Fv, 75.50.Tt

I. INTRODUCTION

A spiral spin density-wave (SDW) structure of fcc-(γ-)Fe was found by Tsunoda about two decades ago using neutron scattering experiments for samples with small pure Fe or FeCo alloy precipitates in a Cu matrix.[1] γ-Fe is a key element and the simplest itinerant electron system with a noncollinear spin structure. Furthermore, various properties of Invar alloys that are important for industrial purposes are greatly indebted to the properties of γ-Fe. Thus, the spiral SDW state of γ-Fe was considered as an ideal test for the application of the first principles calculations to noncollinear itinerant spin systems. Until now, great efforts have been made to reproduce the spiral SDW ground state of γ-Fe by the first principles calculations based on density functional theory. In early studies, Uhl *et al.* and Mryasov *et al.* succeeded in deriving the spiral SDW ground state for γ-Fe in some atomic volume range.[2,3] However, the wave vector of the ground state spiral SDW was around $\mathbf{q}_1=(0.6,0,0)(2\pi/a)$, which is different from the experimental value $\mathbf{q}_2=(1,0.12,0)(2\pi/a)$. Körling and Ergon introduced the generalized gradient approximation (GGA) in their calculations and showed that the new energy minimum appeared at $\mathbf{q}=(1,0.5,0)(2\pi/a)$.[4] Early development of theories on the noncollinear itinerant magnet has been summarized by Sandratskii.[5] Bylander and Kleinman obtained the spiral SDW state with the wave vector very close to the experimental value together with the peak at $(1,0,0)(2\pi/a)$ in their LSDA calculation with a spin stiffness correction.[6] Interestingly, they also derived theoretically that the ground state of γ-Fe is a spiral SDW rather than the collinear SDW as realized in Cr. Taking into consideration of the intra-atomic noncollinearity, Knöpfle *et al.* succeeded in reproducing the spiral SDW with the wave vector of the experimental value using the modified ASW method with GGA and full shape potential, although at a slightly smaller lattice constant.[7] However, this was not the end of the story. Sjöstedt and Nordström performed more precise calculations using the full-potential augmented plane wave method within the GGA.[8] The magnetization was treated as a vector field everywhere in the unit cell. Then, the lowest energy was obtained for a double-layered antiferromagnetic structure with atomic volume identical to Cu. Marsman and Hafner also obtained a spin-spiral ground state with propagation vector at $\mathbf{q}=(0.2,0,1)(2\pi/a)$ with considerably smaller atomic volume than the experimental value.[9] In any case, the theoretical ground state magnetic structure of γ-Fe is very sensitive not only to the atomic volume but also to details of the calculation methods. Many theoretical efforts still keep on searching for the real ground state magnetic structure of γ-Fe.[10–13]

Although several calculations have succeeded in reproducing the spiral SDW state with the propagation wave vector consistent with the experimental results, a common result for these calculations is that the spiral SDW is only stable for atomic volumes smaller than the observed one. In these calculations, except for few authors,[4,8] the lattice was assumed to be an ideal cube even below the Néel temperature. Furthermore, for the cubic structure, theoretical calculations predict that the triple-**Q** spiral structure has the lowest energy.[13] From these calculations, we anticipated that there may be some unknown factors that stabilize the spiral SDW structure realized in the γ-Fe precipitates in Cu. In the present experiments, we took notice of the magnetic symmetry of the spiral SDW structure, which has a tetragonal symmetry or lower.

From the previous experiments, we know that the lattice deformation at the onset of the spiral SDW would rather be small even if it exists. In an ordinary magnetic phase transition with small magnetostriction, a single crystal has usually multiple magnetic domains below the transition temperature under an atmospheric pressure. However, if we apply uniaxial pressure to the single crystal through the transition temperature along the direction parallel to the lattice contraction (say, the c axis), we can obtain a monodomain single crystal with the c axis parallel to the uniaxial stress (the stress cooling). Thus, the relevant magnetic domain occupies the whole volume of the crystal. We can apply this technique to study the existence of the spontaneous magnetostriction at the onset of the spiral SDW ordering of γ-Fe precipitates. Under the atmospheric condition, the precipitates with all possible propagation wave vectors of the spiral SDW are considered to show an equal distribution. However, under the

uniaxial pressure, the distribution of the precipitates with different propagation wave vectors would change if the spontaneous lattice distortion occurs at the onset of the spiral SDW; the numbers of the precipitates would increase with the lattice contraction along the direction parallel to the uniaxial pressure. Thus, to investigate the lattice structure in the spiral SDW state, we performed neutron scattering experiments for the γ-Fe precipitates in Cu under uniaxial pressure.

II. SAMPLE PREPARATION AND MEASUREMENTS

Since pure γ-Fe precipitates that have reached a reasonable size ($d > 30$ nm) in a Cu matrix undergo structural phase transition and show complex magnetic structure below the Néel temperature, they are not suitable for studying the magnetic properties of the spiral SDW. We used $Fe_{97}Co_3$ alloy precipitates for which the structural phase transition is completely suppressed even for the precipitates with the maximum size ($d \sim 150$ nm). The experiment was repeated twice, using different specimens, with $Fe_{97}Co_3$ alloy precipitates. The first attempt was about eight years ago but was not published at that time. After recent development of theories, we completed the experiment again using another sample and obtained consistent results. We refer to the sample used in the old measurements as sample 1 and the one used in the recent measurements as sample 2. Both specimens were single crystals with the composition of $Cu_{97}(Fe_{97}Co_3)_3$, which were grown in the furnace with carbon electrode in Ar atmosphere. After quenching the samples from 1000 °C, precipitation anneal was performed at 725 °C for 20 h, which is considered to be sufficient for observing the well defined SDW satellite peaks. Using the equation derived by Borrelly *et al.*, the averaged particle size of the precipitates is estimated to be 80 nm.[14]

Neutron scattering measurements for both specimens were performed with a T-1-1 triple axis spectrometer installed on the thermal guide of JRR-3M, Tokai, JAEA. To remove higher order contamination, neutrons with a wavelength of 0.245 nm were used together with a pyrolytic graphite (PG) filter. Since the old data for sample 1 still included the higher order contamination of Cu Bragg peaks, the new measurements were carefully performed using a very thick PG filter to eliminate higher order contaminations at the expense of neutron intensity.

Uniaxial pressure was applied along the direction perpendicular to the (0,0,1) scattering plane using a specially designed device with a hard coil spring. The sample was placed on the device and uniaxial pressure was applied, and then, the temperature was lowered using a refrigeration unit. Applied pressure was estimated from the spring constant of the coil spring, which was separately determined by a stress strain machine at room temperature. The pressures applied to sample 1 and sample 2 were 35 and 50 MPa, respectively. Using Young's modulus of Cu (129.8 GPa), induced strains for the Cu matrix were estimated to be 2.7×10^{-4} and 3.9×10^{-4}, respectively. Since γ-FeCo lattices precipitate coherently in the Cu matrix, it would be reasonable to consider that the γ-FeCo precipitates also suffer the same order of strain under the applied uniaxial stress. If we assume that the lattice expands to half the value of the strain in the direction perpendicular to the applied stress, the tetragonality of the lattice induced by the uniaxial pressure is estimated to be of the order of 5×10^{-4}, which is too small to be observed by the neutron triple axis spectrometer with ordinary resolution.

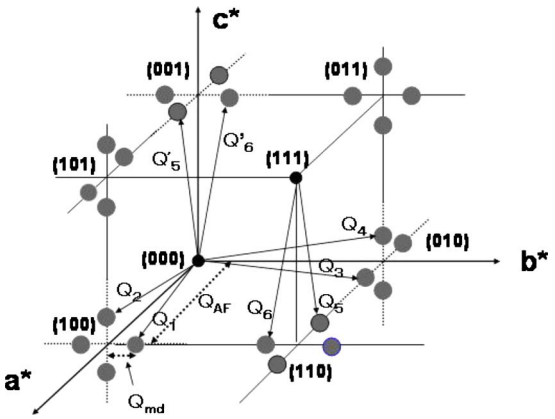

FIG. 1. (Color online) Satellite peak positions in the reciprocal lattice space existing around the original point for a multivariant specimen. Uniaxial stress was applied along the c^* axis and the satellite peaks around the a^*b^* plane were studied.

III. EXPERIMENTAL DATA

From the previous experimental results, the spiral SDW states are classified into six variants under atmospheric conditions. (For a single crystal magnet, these "variants" should be called as magnetic domains, but in the present case, small particles of γ-$Fe_{97}Co_3$ alloy coherently precipitate in a Cu single crystal. Each particle orders to the spiral SDW state with one of the SDW wave vectors at low temperature. Here, we have used the term variants for precipitates with the spiral SDW of different wave vectors in a specimen.) Although some theories predict the multiple SDW state as the ground state of cubic γ-Fe,[13] here we assume the single-**Q** SDW state because in neutron scattering measurements, we cannot distinguish the multiple SDW and multivariant single-**Q** SDW state with equal distribution of the variants. Then, each variant shows the satellite peak of a spiral SDW state defined by a wave vector **Q** in the reciprocal lattice space. Under ambient pressure, all variants of the SDW are formed with equal probability below the Néel temperature. All of the satellite peak positions appearing around the original point are schematically illustrated in Fig. 1. In this figure, the contribution from each SDW variant is designated by $\mathbf{Q}_i$ ($i = 1-6$). In the present measurements, all of the satellite peaks observable around the (0,0,1) scattering plane were studied with and without uniaxial pressure applied along the direction perpendicular to the scattering plane. In this condition, the satellite peaks at $\mathbf{Q}_1$, $\mathbf{Q}_3$, $\mathbf{Q}_5$, and $\mathbf{Q}_6$ are located on the (0,0,1) scattering plane, but those at $\mathbf{Q}_2$ and $\mathbf{Q}_4$ are slightly away from the exact scattering plane. The satellite peaks for $\mathbf{Q}_2$ and $\mathbf{Q}_4$ were studied by step scanning with a tilting angle of the goniometer with fixed counter angle. All of the data were taken at the lowest temperature of the re-

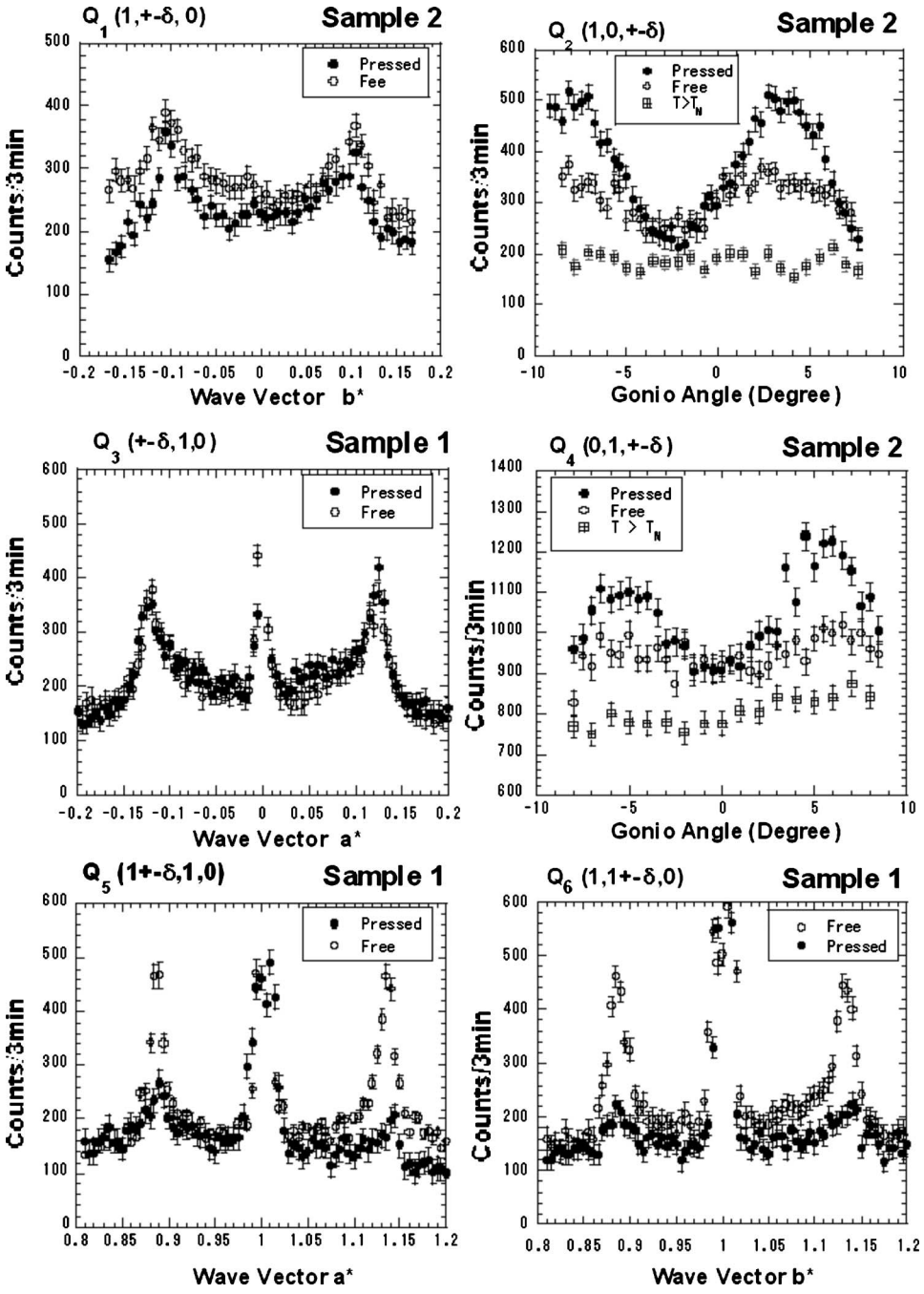

FIG. 2. Line profiles obtained at each satellite peak position studied with and without uniaxial stress. The central peak observed for sample 1 is a higher order contamination of Cu Bragg peak owing to imperfect filtering. For sample 2, higher order contamination was carefully removed using a thick filter. The peak shift of the $\mathbf{Q}_2$ satellite is because of missetting of the crystal axis.

frigerator (10–12 K), which is far below the Néel temperature of the samples (30 K). Examples of the data obtained for sample 1 and sample 2 are given in Fig. 2. The central peaks observed for sample 1 were higher order contaminations of Cu Bragg peaks due to insufficient filtering. Thus, for sample 2, higher order components were carefully removed using a thick filter at the cost of intensities. Since a vertical focusing monochromator was used in this spectrometer with no horizontal collimators, the resolution of the spectrometer for the direction perpendicular to the scattering plane was rather poor and the line profiles for the $\mathbf{Q}_2$ and $\mathbf{Q}_4$ satellites were very broad. In spite of small lattice distortion induced by the applied uniaxial stress, drastic changes in the scattering intensities were observed for some satellite peaks. For the $\mathbf{Q}_2$ and $\mathbf{Q}_4$ satellites, the peak intensities strongly increased under uniaxial stress, and for the $\mathbf{Q}_5$ and $\mathbf{Q}_6$ satellites, they decreased remarkably, while the $\mathbf{Q}_1$ and $\mathbf{Q}_3$ satellites did not show marked changes in intensities. The changes in the satellite peak intensities by the applied uniaxial stress are schematically illustrated in Fig. 3.

From these data, we can obtain common rules. Let us rewrite the satellite wave vector $\mathbf{Q}_i$ as the sum of $\mathbf{Q}_{\mathrm{AF}}$ and $\mathbf{Q}_{\mathrm{md}}$ as shown in Fig. 1,

$$\mathbf{Q}_i = \mathbf{Q}^i_{\mathrm{AF}} + \mathbf{Q}^i_{\mathrm{md}} \quad (\mathbf{Q}^i_{\mathrm{AF}} \perp \mathbf{Q}^i_{\mathrm{md}}),$$

where $\mathbf{Q}^i_{\mathrm{AF}}$ is a propagation vector of the nearest-neighbor antiferromagnetic coupling and parallel to the cubic axis, and $\mathbf{Q}^i_{\mathrm{md}}$ is a propagation vector of spin modulation that has a

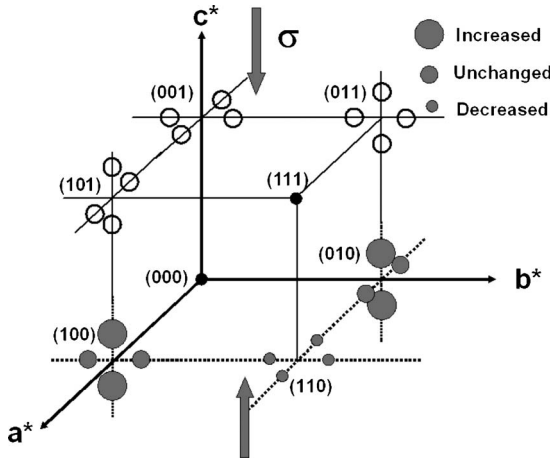

FIG. 3. Schematic illustration showing changes in the satellite peak intensities under uniaxial stress applied along the c^* axis.

long period and is incommensurate with the lattice periodicity. Strictly speaking, the $\mathbf{Q}^i_{\mathrm{AF}}+\mathbf{Q}^i_{\mathrm{md}}$ and $\mathbf{Q}^i_{\mathrm{AF}}-\mathbf{Q}^i_{\mathrm{md}}$ satellite peaks come from different variants (clockwise rotation and anticlockwise rotation) for a helical spin structure. However, in the present measurements, both peaks always behave in the same way and we treat them as the same variant. If we express the uniaxial stress as $\boldsymbol{\sigma}$, then all data are consistently explained by the following rules.

(1) The satellite intensities with $\mathbf{Q}^i_{\mathrm{md}}$ parallel to $\boldsymbol{\sigma}$ increase with applied uniaxial stress.

(2) The satellite intensities with $\mathbf{Q}^i_{\mathrm{AF}}$ parallel to $\boldsymbol{\sigma}$ decrease with applied uniaxial stress.

Since the lattice is considered to contract in the direction parallel to $\boldsymbol{\sigma}$ and expand in perpendicular directions, both effects are canceled for the satellite intensities of $\mathbf{Q}_1$ and $\mathbf{Q}_3$ variants, with the result that the peak intensities retain unchanged.

Although the satellite peak intensities changed drastically under the applied uniaxial pressure, the satellite peak positions and line profiles did not change within the experimental errors.

Since an fcc antiferromagnet is a typical spin frustration system, breakdown of cubic symmetry by the applied uniaxial stress may lead to increased Néel temperature. It was, however, difficult to study this point because the pressure device had a large heat capacity, and it took a long time to reach the thermal equilibrium of the device around the Néel temperature.

After completing neutron scattering measurements, the coherence of the lattice of γ-FeCo precipitates with Cu matrix was checked by x-ray diffraction for sample 1 at room temperature. No change of the sample situation had occurred after the uniaxial stress measurements.

IV. DISCUSSION

Changes of magnetic satellite peak intensities under uniaxial stress may be explained by the change in the spin structure. However, it was difficult to consider an actual spin structure, which can explain the observed changes in the satellite peak intensities consistently. Absence of changes in the $\mathbf{Q}_1$ and $\mathbf{Q}_3$ satellite peak intensities would evidence that the spin structure did not change. In the present paper, from an analogy with the stress cooling of a conventional magnetic substance with magnetostriction, we assumed that changes in the satellite peak intensities were ascribed to those of the volume fractions between variants. Increase in the satellite peak intensities of some variants under uniaxial pressure indicates that numbers of precipitates increased with the lattice contraction along the direction parallel to the uniaxial pressure and that the fcc lattice spontaneously contract along the relevant direction at the onset of the spiral SDW ordering. Then, we can conclude that the cubic γ-$Fe_{97}Co_3$ lattice contracts along the $\mathbf{Q}_{\mathrm{md}}$ direction and expands along the $\mathbf{Q}_{\mathrm{AF}}$ direction at the onset of the spiral SDW ordering. Furthermore, the results indicate that the magnitude of the lattice deformations is comparable order to the external lattice deformation ($\sim 10^{-4}$), because if the spontaneous lattice deformation is of an order of magnitude smaller (larger) than that induced by the uniaxial stress, the influence induced by the uniaxial stress would be more (less) effective. Existence of spontaneous lattice deformation under ambient pressure is supported by our earlier x-ray diffraction data in which the (4,0,0) Bragg peak intensity slightly decreased below the Néel temperature (see Fig. 1 of Ref. 1). The magnitude of the lattice deformation is consistent with the value determined from the shift of the Bragg peak position (4×10^{-4}).[1] The direct observation of the lattice deformation and symmetry at the onset of the spiral SDW ordering using high-resolution x ray will be considered in a future study.

As for the lattice symmetry that stabilizes the spiral SDW state, the similarity with a CuMn spin-glass alloy should be noted. The CuMn alloy had been regarded as a prototypical spin-glass system, and it was thought that Mn spins freeze in random directions without any spatial spin correlation below the freezing temperature. However, Cable *et al.* discovered magnetic diffuse peaks at the $1,1/2\mp\eta,0$ and equivalent symmetry positions of the reciprocal lattice space (RLS) using polarized neutron scattering, indicating that Mn spins freeze with magnetic short range order (SRO) of an incommensurate spin structure.[15] Note that these peak positions have the same symmetry as the satellite peaks observed for the cubic γ-Fe precipitates in Cu. Thus, the SDW wave vector $\mathbf{Q}$ of CuMn alloy is also written as $\mathbf{Q}=\mathbf{Q}_{\mathrm{AF}}+\mathbf{Q}_{\mathrm{md}}$, although the magnitude of $\mathbf{Q}_{\mathrm{md}}$ (wave vector of spin modulation) is different from that in the γ-Fe precipitates. Cable *et al.* showed that the each satellite diffuse peak of CuMn alloys has an ellipsoidal distribution elongated along the $\mathbf{Q}_{\mathrm{AF}}$ direction in the RLS, i.e., the spin correlation length along the $\mathbf{Q}_{\mathrm{AF}}$ direction is shorter than those along the other two directions.[15] Later, using neutron scattering, Tsunoda and Cable studied the CuMn alloy single crystal with highly developed atomic short range order[16] (ASRO) and found that the CuMn alloy with well-developed ASRO shows very sharp magnetic satellite peaks and the lattice elongates along the direction parallel to the $\mathbf{Q}_{\mathrm{AF}}$ vector (in Ref. 16, $\mathbf{Q}_{\mathrm{AF}}//c$ axis and $\mathbf{Q}_{\mathrm{md}}//b$ axis). These data indicate that the SDW of CuMn alloys is stabilized by the atomic order and that the lattice parameter along $\mathbf{Q}_{\mathrm{AF}}$ is longer than that along $\mathbf{Q}_{\mathrm{md}}$. For an ordinary CuMn spin-glass alloy, the ASRO does not

develop sufficiently and the lattice retains a cubic structure, resulting in the SRO of the SDW. The reason why the spin correlation length along the $\mathbf{Q}_{AF}$ direction is very short for an ordinary CuMn spin-glass alloy may be because of the constraint of the cubic lattice for a sample with poorly developed ASRO. Thus, the spiral SDW state for cubic γ-Fe has the same lattice symmetry as that of the CuMn alloy and most likely the same magnetic structure.

It would be interesting to compare the present results with the sinusoidal SDW system Cr. In the case of Cr, a charge density wave accompanied by the SDW ordering was observed, and this induces a local strain wave with an amplitude of the order of 10^{-3}.[17,18] Since the strain wave itself is a wavy modulation, it does not induce uniform lattice expansion. However, Steinitz *et al.* observed uniform lattice expansion of the order of 10^{-6} for the direction parallel to $\mathbf{Q}_{md}$ (in the SDW of Cr, $\mathbf{Q}_{md}//\mathbf{Q}_{AF}$) just below the Néel temperature, and the lattice contraction was found to be far below the Néel temperature.[19] On the other hand, no strain waves were observed for the γ-FeCo SDW states within the experimental error ($I_{SW}/I_{220}<2.3\times10^{-5}$), which is of the same order of the strain wave in Cr.[1] This is an experimental evidence for the spiral spin structure model of cubic γ-Fe. Thus, the lattice deformation for γ-FeCo precipitates is completely different from that of Cr.

The first principles calculations for the spiral SDW state of γ-Fe in the tetragonal lattice were first performed by Körling and Ergon[4] and then by Marsman and Hafner[9] in detail. They treated the tetragonal lattices of the order of 10^{-2}, which is far greater than that observed here, but their results showed that the introduction of tetragonal lattice distortion to the spiral SDW state is not helpful in solving the inconsistency between theoretical calculations and experimental data except for the cases with very small volume. Their works should rather be applied to the γ-Fe thin films epitaxially grown on the appropriate substrate or the large γ-Fe precipitates for which the cubic structure becomes unstable and the structural phase transition with percent order of lattice distortion that takes place at the onset of magnetic ordering. Although the calculated ground state energies for the spiral SDW state in γ-Fe are very sensitive to the atomic volume, since the lattice distortion at the onset of spiral SDW state for γ-Fe precipitates is very small, it is doubtful whether the introduction of lattice distortion with the extent of observed values would be helpful in solving the discrepancies between theoretical calculations and experimental data.

V. CONCLUSION

Using neutron scattering experiments under uniaxial pressure, the lattice symmetry of γ-FeCo precipitates in Cu was studied in the spiral SDW state. Under uniaxial pressure of about 50 MPa applied along the [0,0,1] axis, the total volume of the precipitates with $\mathbf{Q}_{md}$ vector parallel to the [0,0,1] axis increased and that with $\mathbf{Q}_{AF}$ vector decreased, indicating that the fcc lattice contracts along the $\mathbf{Q}_{md}$ direction and expands along the $\mathbf{Q}_{AF}$ vector at the onset of spiral SDW ordering. Thus, the γ-Fe lattice deforms to a tetragonal or orthorhombic structure below the Néel temperature. The magnitude of lattice deformation is estimated to be of the order of 10^{-4}, which would be too small to solve the discrepancies between results obtained from experiments and those from first principles calculations assuming the ideal cubic lattice.

[1] Y. Tsunoda, J. Phys. F: Met. Phys. **18**, L251 (1988); J. Phys.: Condens. Matter **1**, 10427 (1989).
[2] M. Uhl, L. M. Sandratskii, and J. Kübler, J. Magn. Magn. Mater. **103**, 314 (1992).
[3] O. N. Mryasov, V. A. Gubanov, and A. I. Liechtenstein, Phys. Rev. B **45**, 12330 (1992).
[4] M. Körling and J. Ergon, Phys. Rev. B **54**, R8293 (1996).
[5] L. M. Sandratskii, Adv. Phys. **47**, 91 (1998).
[6] D. M. Bylander and L. Kleinman, Phys. Rev. B **60**, R9916 (1999).
[7] K. Knöpfle, L. M. Sandratskii, and J. Kübler, Phys. Rev. B **62**, 5564 (2000).
[8] E. Sjöstedt and L. Nordström, Phys. Rev. B **66**, 014447 (2002).
[9] M. Marsman and J. Hafner, Phys. Rev. B **66**, 224409 (2002).
[10] P. Kurz, F. Förster, L. Nordström, G. Bihlmayer, and S. Blügel, Phys. Rev. B **69**, 024415 (2004).
[11] V. M. Garcia-Suarez, C. M. Newman, C. J. Lanbert, J. M. Pruneda, and J. Ferrer, Eur. Phys. J. B **40**, 371 (2004).
[12] S. Shallcross, A. E. Kissavos, S. Sharma, and V. Meded, Phys. Rev. B **73**, 104443 (2006).
[13] T. Uchida and Y. Kakehashi, J. Phys. Soc. Jpn. **75**, 094703 (2006).
[14] R. Borrelly, J. M. Pelletier, and E. Pernoux, Scr. Metall. **9**, 747 (1975).
[15] J. W. Cable, S. A. Werner, G. P. Felcher, and N. Wakabayashi, Phys. Rev. B **29**, 1268 (1984).
[16] Y. Tsunoda and J. W. Cable, Phys. Rev. B **46**, 930 (1992).
[17] Y. Tsunoda, M. Mori, N. Kunitomi, Y. Teraoka, and J. Kanamori, Solid State Commun. **14**, 287 (1974).
[18] E. Fawcett, Adv. Phys. **60**, 228 (1988).
[19] M. O. Steinitz, L. H. Schwartz, J. A. Marcus, E. Fawcett, and W. A. Reed, Phys. Rev. Lett. **23**, 979 (1969); J. Appl. Phys. **41**, 1231 (1970).